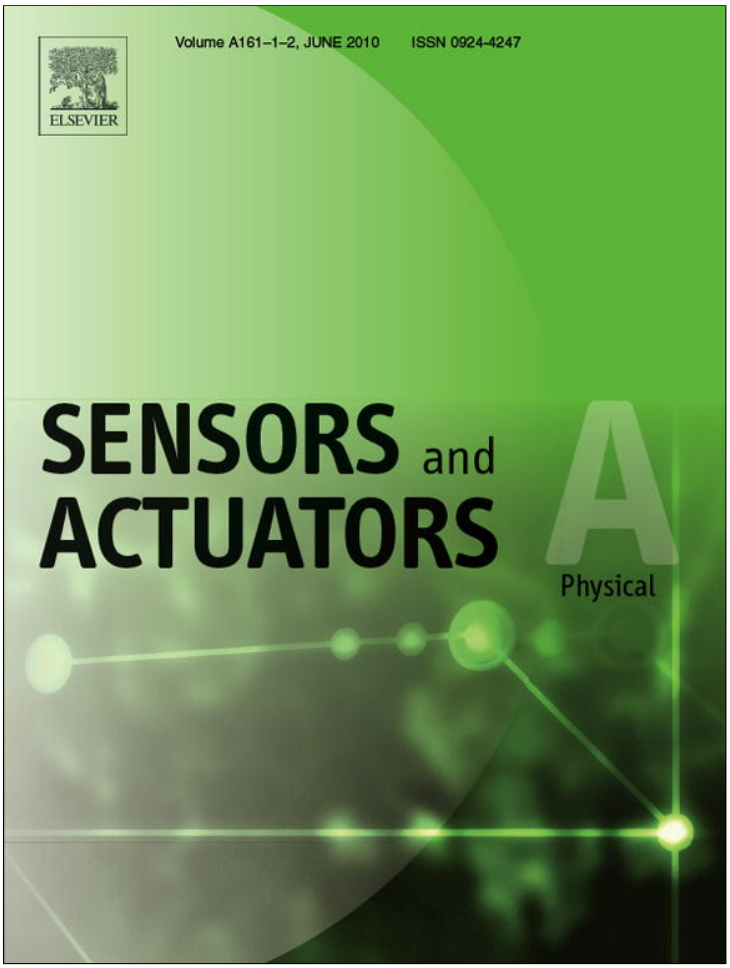

Sensors and Actuators A 161 (2010) 108–113

Contents lists available at ScienceDirect

Sensors and Actuators A: Physical

journal homepage: www.elsevier.com/locate/sna

A micro-machined Pirani gauge for vacuum measurement of ultra-small sized vacuum packaging

Xuefang Wang[a,c], Chuan Liu[b], Zhuo Zhang[a,c], Sheng Liu[a,c], Xiaobing Luo[b,c,*]

[a] School of Mechanical Engineering, Huazhong University of Science and Technology, Wuhan 430074, China
[b] School of Energy and Power Engineering, Huazhong University of Science and Technology, Wuhan 430074, China
[c] MOEMS Division, Wuhan National Lab for Optoelectronics, Huazhong University of Science and Technology, Wuhan 430074, China

ARTICLE INFO

Article history:
Received 8 December 2009
Received in revised form 30 April 2010
Accepted 30 April 2010
Available online 7 May 2010

Keywords:
Wafer level
Vacuum packaging
Pirani gauge
Vacuum monitor

ABSTRACT

Quite a few MEMS devices need vacuum packaging technology to guarantee the desirable performance. Developing an absolute vacuum environment for those devices is indispensable. However, it is difficult to monitor the pressure change in vacuum chamber in on-line and real-time mode. A surface micro-machined Pirani gauge for measuring vacuum pressure inside vacuum packaging in wafer level was presented in this paper. It was designed with a simplified structure and did not need complex circuit. Only a simple Wheatstone bridge circuit is needed, which could be manufactured by conventional CMOS processes. Preliminary tests on this device were conducted. The experimental results show that the Pirani gauge is capable of measuring pressures from atmospheric value to 1 Pa and has a very good linearity in the range from1 Pa to 300 Pa. It demonstrates that the micro-machined Pirani gauge has great potential to be used in wafer level vacuum packaging. Also, the Pirani gauge is able to be the packaging hermeticity detector.

1. Introduction

In recent years, numerous devices require vacuum packaging for optimal operation [1], such as MEMS gyroscope sensors, micro-filters, MEMS ultrasonic sensors [2,3], high-end micro-accelerometers [4,5] and so on. These devices need vacuum environments to reduce the gas damping of the mechanical moving parts, which will improve the device quality factor, enhance their performances, and greatly reduce the energy consumption of the whole microsystem.

Existing methods for vacuum measurement in MEMS devices include helium leak testing and Q factor extraction [6,7]. Helium leak testing needs expensive equipment (~$15,000) and is generally limited to the application situations where the leak rates are greater than 10^{-12} cm^3/s [1]. The above factor results in high cost and cannot perform on-line and real-time pressure change observation in vacuum cavity for helium leak testing. Q factor measurements are limited by complicated circuits and not sufficient sensitivity at the level of low pressures [8,9], thus, it cannot precisely measure small pressure change inside a sealed micro-cavity [10]. Our group reported on-line monitoring method using embedded resonator [11,12]. However, for these sensors, their fabrications are complicated and expensive, and they are proved to have low pressure sensitivity under 10 Pa.

So far, numerous miniaturized Pirani gauges have been reported due to the development of micro-machining technology [13,14], which can utilize simple front-surface-etching technique and provides wide and linear response [15]. In addition to these devices, a new surface micro-machined Pirani pressure sensor with an extremely narrow gap between heater and heatsink (substrate) was also designed and fabricated in reference [16].

In this paper, a low cost and high sensitivity micro-machined vacuum gauge – Pirani gauge – was presented, which is suspended by a thin membrane structure, with a groove cavity etched on the substrate. The heater material is Pt, it has good linearity and stability. Compared with traditional structure of four supporting beams, the present structure provides not only low thermal loss through leads to the substrate and large active area for gaseous heat conduction, but also can strengthen mechanical support for the Pirani vacuum sensor. Meanwhile, it can be integrated with general micro-packaging technologies. Experimental tests on this Pirani gauge were conducted. The experimental results show that this Pirani gauge is capable of measuring a range of pressures linearly from atmospheric to 1 Pa and has a very good linearity especially in the range of 1–300 Pa.

* Corresponding author at: School of Energy and Power Engineering, Huazhong University of Science and Technology, Wuhan 430074, China.
E-mail address: Luoxb@mail.hust.edu.cn (X. Luo).

0924-4247/$ – see front matter © 2010 Elsevier B.V. All rights reserved.
doi:10.1016/j.sna.2010.04.034

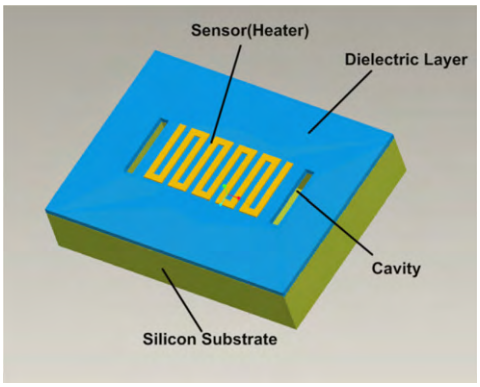

Fig. 1. Device structure of micro-Pirani sensor.

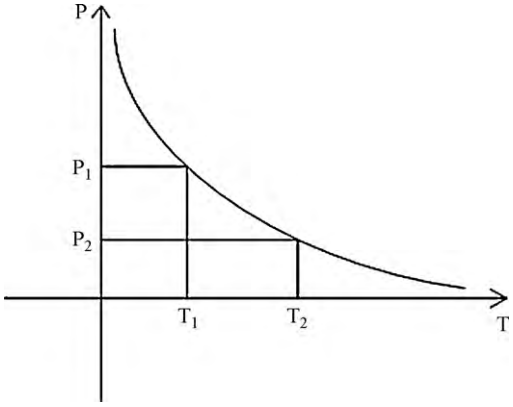

Fig. 2. Profile of vacuum chamber's pressure versus temperature.

2. Device structure and operation principle

Fig. 1 shows the device structure of the present micro-Pirani sensor. It includes a cavity, an insulating layer locally positioned on the cavity and the sensor deposited on the insulating layer such that the air moves across the sensors by virtue of free convection. The sensor acts as the heater during operation.

Pirani gauge's working principle is based on the fact that heat loss of a hot plate to its ambient through gas conduction is proportional to the molecular density of gas in the vacuum system [17]. The vacuum pressure can be measured in terms of the temperature changes of the platinum film sensitive resistor, which is reflected accurately by the amount of heat loss. The device is packaged in a sealed vacuum chamber. When the sensor is provided with a current, its temperature rises, then the air around it is heated, free convection is established in the cavity. The output current changes as temperature changes, by measuring the current difference, the pressure of the vacuum chamber can be acquired.

Fig. 2 shows the profile of the vacuum chamber's pressure versus temperature. From the figure it can be seen that the temperature of the platinum film sensitive resistor changes at the same time when the vacuum pressure of the vacuum chamber changes. Thus the resistance changes with the changed temperature, the vacuum pressure can be obtained through measuring the output voltage.

3. Design

The input power to the MEMS Pirani sensor is equal to the heat loss of heater to its ambient, the main heat transfer includes solid conduction, gas conduction, and thermal radiation. The magnitude of each term depends on the structure and the ambient conditions.

For pressure measurement, the major contributions come from the term of the gaseous conduction, which can be expressed as [15,17]

$$G_g = \frac{\varphi}{2-\varphi} G_a A_s P \left(\frac{P_{t1}}{P+P_{t1}} + \frac{P_{t2}}{P+P_{t2}} \right) \quad (1a)$$

and

$$G_a = \Lambda_0 \left(\frac{273.2}{T_a} \right)^{1/2} \quad (1b)$$

where φ is the accommodation coefficient of gas; G_a and Λ_0 are the free molecular conductivities at T_a and at 273 K, respectively; As is the floating plate area; P is the ambient pressure; P_{t1} and P_{t2} are transition pressures on both sides of the membrane, which are inversely proportional to the effective separations of the membrane from their heat sinks [17].

For the thermal conduction of the present device, it can be assumed that the temperature distribution is mainly determined by the contact area of heated film and the insulating layer, the physical and geometric properties of the insulating layer. An empirical formula for the thermal conduction of the device was reported previously by Weng and Shie [15], which is written as

$$G_s = \left(\frac{1}{4.2 k_t d} \frac{B}{A} + 5 \times 10^4 \right)^{-1} \quad (2)$$

where k_t is the thermal conductivity (W/cm °C), d is the effective thickness of the glass with its Pt-coated film. The first term on the right-hand side of Eq. (2) is the thermal resistance of the leads. The second term represents the spreading resistance on the membrane area. In the design, the membrane is treated as uniform material having an equivalent thermal conductivity of 0.0312 W/cm °C and an equivalent thickness of 250 nm. Here A = 100 μm and B = 477 μm. Conductivity of the platinum film is estimated from its bulk value. Real conductivity, however, is generally lower due to the effect of surface scattering of thin films [15].

Regarding to the radiation heat transfer of a floating membrane, the Stefan–Boltzmann law is used, which results in the following equation [15,18]:

$$G_r = 2\varepsilon\sigma A_s \left(T^2 + T_a^2 \right) (T + T_a) \quad (3)$$

where ε is the emissivity, A_s is the floating plate area, and σ is the Stefan–Boltzmann constant.

From the above analysis it is known that the increasing of the gas convection heat transfer and reducing thermal conduction can increase the sensitivity and the dynamic range of the Pirani gauge. In this paper, we used two measures to realize the above target, the first is that a groove cavity is etched in the substrate to reduce the contact area of the dielectric layer with the substrate, the second is to reduce the thickness of dielectric layer and choose some insulation materials with small thermal conductivity.

Using Eqs. (1)–(3), we have designed numerous dimensions to try to achieve the best performance. Every dimension can use the above equations to calculate, and by comparing the results of thermal distribution at different designs, we can get the optimum dimensions.

Fig. 3 shows the calculation results of the thermal conductance for one design. In Fig. 3, the total thermal conductance, G_t, is the sum of the above three quantities in Eqs. (1)–(3). Λ_0 is 0.0164 W/cm^2 °C, and the parameters φ, P_{t1} and P_{t2} are 0.9, 19.72, and 1.12 [15]. When the air pressure is larger than 100 Torr, G_g is approximately four times of G_s, and is nearly saturated. G_g decreases linearly with the vacuum pressure when it is smaller than 10 Torr. The radiative conductance of the device shown here is obtained by assuming that the temperature rise of the plateau is 100 °C or more at zero-pressure condition for the ambient. It decreases slightly in the high-pressure regime.

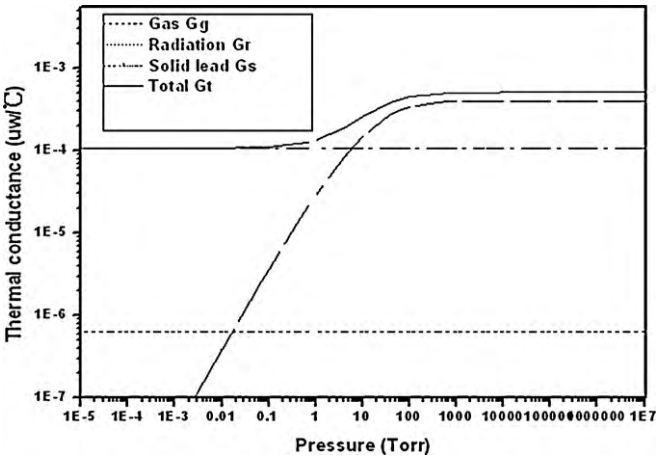

Fig. 3. Various thermal conductance dependences on pressure.

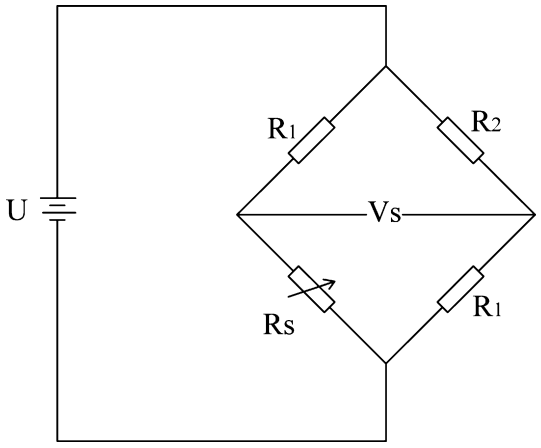

Fig. 6. Wheatstone bridge circuit for Pirani gauge readout.

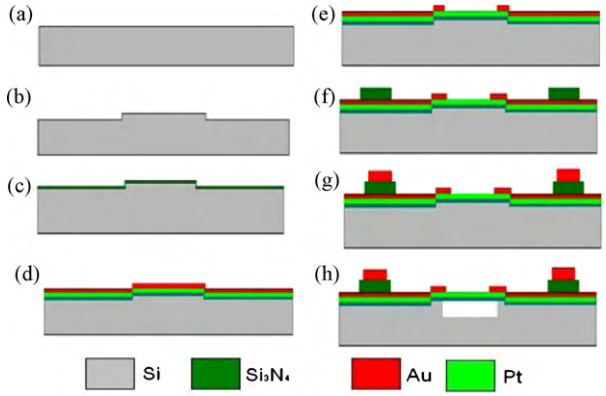

Fig. 4. Processes for fabricating Pirani gauge.

Based on the above optimization process, the sensor is finally designed as a square structure with the length of 5897 μm and the width of 10 μm. It includes 10 segments, and the distance between each single resistor segment is 20 μm. Therefore, the sensor has a square structure with dimensions 571 μm × 280 μm × 0.25 μm.

4. Fabrication

The device is fabricated by surface micro-machining processes as shown in Fig. 4. It is summarized as follows: (a) Preparing a thermally oxidized n-type, 100 oriented silicon wafers. (b) The 1 μm deep cavity is etched on the wafer and patterned by the metal electrode and the resistor. (c) The 1 μm thick Si_3N_4 membrane layer is deposited on the cavity by PECVD, which can reduce total intrinsic stress efficiently and obtain lower solid thermal conductivity [14]. (d) The 0.25 μm thick Cr/Pt resistor with sheet resistance 550–650 Ω is deposited and patterned using PVD followed by Cr/Au metal electrode that is sputtered to connect the meander resistor. (e) The part of the Cr/Au metal electrode which is above the meander resistor is eroded to expose the resistor. (f) After eroding, the 0.5 μm Si_3N_4 by PECVD is deposited and patterned. (g) The metal bonding layer is deposited and patterned. (h) Then etch-windows are opened. At last, the substrate is released in wet etch and dried in volatile organic solvent. Fig. 5 is the photomicrograph of the device that is exposed in atmosphere.

5. Experimental test

For Pirani gauges, constant temperature circuits (CT) are usually used for that they can protect the sensor from overheating and provide the sensor a wide measuring range, but they are generally complicated and require a rigorous implementation. Therefore, constant current bias (CC) and the Wheatstone bridge configuration are also widely used in many commercial Pirani gauges [14]. In our measurements, the fabricated sensor is driven by conventional Wheatstone bridge circuit, as shown in Fig. 6, where R_s is the sensor, and R1, R2 are made of the same material with the same resistance. The linear constant voltage sources were used as the power, and the output voltage is measured by a digital multimeter.

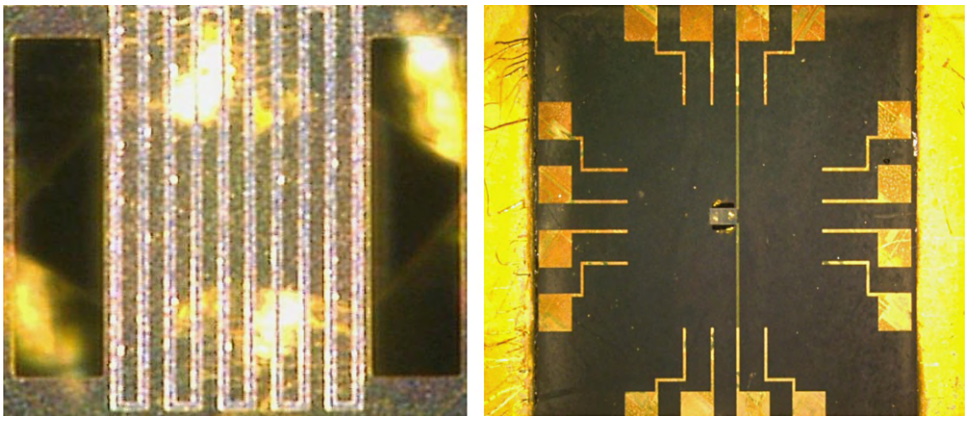

Fig. 5. Microscope photograph of the structure.

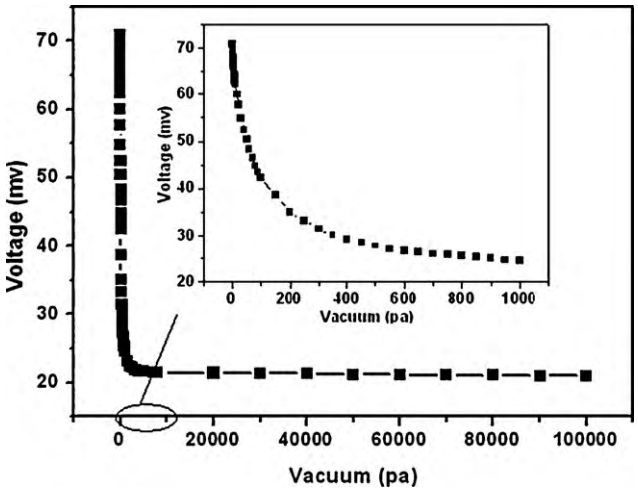

Fig. 7. Curve of the voltage versus vacuum.

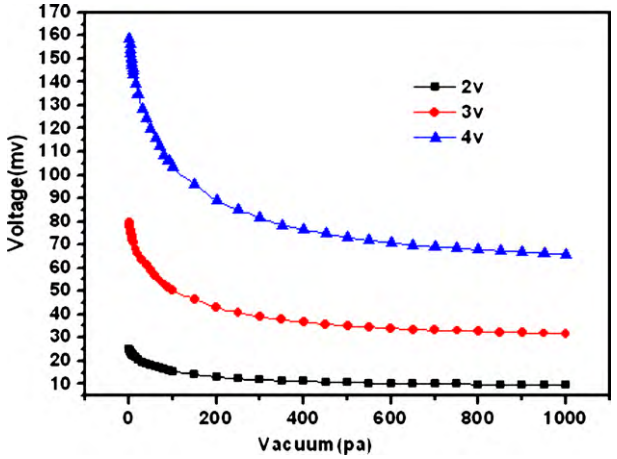

Fig. 8. Curve of voltage versus vacuum under different voltage.

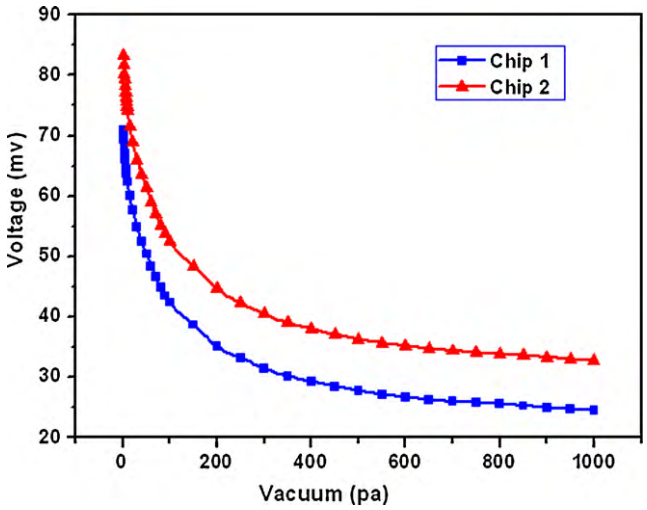

Fig. 9. Voltage versus vacuum under different chip.

When the heat loss of the heater sensor to its ambient is different under diverse vacuum pressures, the temperature of the platinum film resistance changes simultaneously, the value of the platinum film resistance will change according to the resistivity and temperature-related features, and eventually lead to changes of the output voltage in the Wheatstone bridge circuit. The vacuum system used for the measurements is available in the pressure range from 1 Pa to atmosphere. The sensor fixed in the square chamber connects with the circuits outside. The first measurement procedure is to pump the system below 1 Pa, then slowly open the valve to bleed the gas into the chamber to obtain the desired pressure, and real-time output voltages of the circuits are measured with a digital multimeter. The curve of the voltage versus vacuum has been achieved by the experiment. The curves are shown in Fig. 7. When we use the Pirani gauge to measure the vacuum pressure, observe the data, and compare them with the calibration curves, the vacuum pressure of the vacuum chamber can be obtained finally.

6. Results and discussion

Fig. 7 shows the curve of output voltage versus pressure. It is found that the output voltage response signals decrease with the increasing of gas pressure in the sensitive range and the fabricated device has a good linearity in the range of vacuum pressure between 1 Pa and 100 Pa. From Fig. 7 we can know that the pressure sensitive range is from 1 Pa to 10^5 Pa. The lowest detectable pressure is nearly 1 Pa. In our previous works [12], we have reported the method of using embedded resonator for on-line monitoring. Their results showed that sensitivity will decrease in the lower vacuum pressure. From Fig. 4, it was found that the sensitivity was very low between 1 Pa and 10 Pa, the curve is nearly flat. But in this paper, from Fig. 7, we can find that the Pirani gauge has a very good linearity in the range from 1 Pa to 100 Pa, it means that it can detect very small pressure, thus the sensitivity is high.

Two Pirani gauges are tested in calibration experiments, marked chip 1 and chip 2, with a resistance of 634 Ω and 607 Ω, respectively.

The calibration curve of the voltage versus vacuum for chip 1 is shown in Fig. 8. In this figure, three different cases were tested. In each case, the input voltage of the heater sensor is different. From Fig. 8, it is found that in the range of vacuum pressure between 1 Pa and 1000 Pa, the linearity under 3 V input voltage is much better than the case with 2 V input voltage and almost the same trends with case of 4 V. When heating voltage changes from 2 V to 4 V, the average voltage signal of the fabricated sensors elevation is about 94.8 mV. Whereas the voltage increase is about 15.6 mV, 47.8 mV and 93 mV of the chip in different heating voltage in the vacuum range, respectively. From Fig. 8, it is found that the sensor has better performance under 3 V input voltage case, this can be explained as following. When the input voltage is 3 V, the temperature of the membrane is about 74.1 °C, which is the maximal work temperature of the Pt membrane sensor. When the temperature is higher than this, the film resistance will be changed and irreversible because of intermetallic compound produced in the film surface at high temperature. We have conducted experiment under 6 V voltage, and the result approved the above conclusions. So the next work is to deposit some inertial metals like Ti or Ni between Pt and Au, this could solve this problem and increase the sensor operation temperature.

Meanwhile, we have calibrated the chip 1 and chip 2 in voltage 3 V, which are shown in Fig. 9. It is known that the linearity of chip 2 is much better than the chip 1.

From Fig. 9 it can draw a conclusion that a common curve for each Pirani gauge with different resistances is necessary. To establish the repeatability of gauge measurements under different conditions, quite a few Pirani gauges were tested. Fig. 9 shows the results of the tests. The resistances of those gauge varied in a range from 550 Ω to 700 Ω.

From the measured results in Fig. 10, the voltage signal of the fabricated sensor versus pressure is obtained when the heating voltage is 3 V. It is clear that each Pirani gauges have similar curves

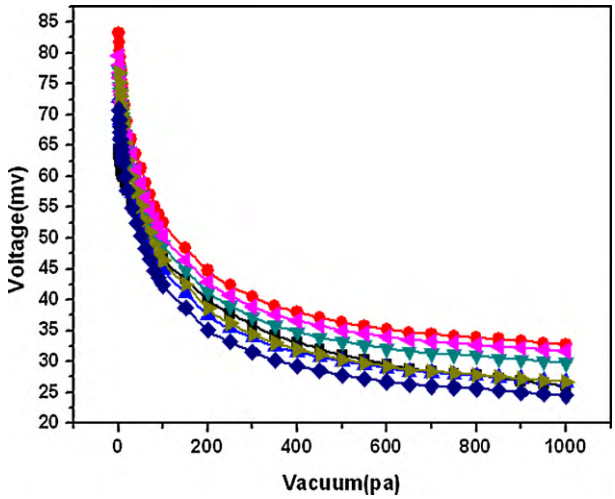

Fig. 10. Curves of voltage versus vacuum under different chips.

Fig. 11. Helium bomb chamber.

and the experiments are repeatable. However, we could not find a current curve for each different Pirani gauge and the voltage versus pressure curve of each Pirani gauge does not have similar order as the value of resistance increase.

Based on the above discussions, we can know that the Pirani gauge can also detect the leak rate of the hermetical packaging of MEMS devices. To prove this point, we also conducted the relative experiments. In the experiment, for the tested Pirani gauge, the input voltage was 3 V, the output voltage was about 21 mV. According to the test data shown in Fig. 7, we know that the detected pressure by Pirani gauge is nearly at atmospheric pressure. This demonstrates that the experimental packaging sample is in leak situation. Actually, this gauge was packaged by Au–Si eutectic bonding in vacuum environment, and we measured the pressure immediately after bonding. If the bonding is successful, the initial pressure will be very low. But in our experiments, for some unclear reasons, the bonding of some of the chips failed and they leaked seriously.

To prove the test result obtained by the Pirani gauge sample, the conventional methods by bubble test and helium bomb test were used to measure the leak rate of hermetical packaging of the same device. In this experiment, the packaged chip was placed in the helium bomb chamber for 2 h, as shown in Fig. 11, then it was

Fig. 12. Helium mass spectrometer.

Fig. 13. Bubble detector.

took out and placed into the helium mass spectrometer, as shown in Fig. 12, the leak rate detected by helium mass spectrometer is about 5.8×10^{-9} Pa m^3/S, this result shows the packaged chip is in serious leak situation. In order to assure the result, we put the packaged chip in bubble detector, as shown in Fig. 13, little bubbles can be seen rising from the detect fluid, this means the packaged chip is leaky.

This test result shows good agreement with the Pirani gauge results. So this Pirani gauge is able to measure the packaging hermeticity. Compared with the conventional method, Pirani gauge is simple, fast and easy to realize real mode test.

7. Conclusions

In this paper, a sensitive MEMS Pirani sensor was proposed. This micro-machined Pirani gauge has great potential for being used for wafer level vacuum packaging. It has been proven that each Pirani

gauge has its own calibration curve, and the calibration curves are also different under diverse input voltages. The Wheatstone bridge circuit is used, which provides a feasible method for improving the performance of the sensors. The experimental results show that the proposed Pirani gauge is capable of on-line and real-time measuring pressures linearly from atmospheric to 1 Pa and has a good linearity in the range of 1–300 Pa. In addition, it is proven by the comparison experiment that the present Pirani gauge is able to be a packaging hermeticity detector.

Acknowledgement

This work was supported by the National High Technology Research and Development Program of China (Program 863) under Grant No. 2008AA04Z307.

References

[1] B.H. Stark, Y. Mei, C. Zhang, K. Najafi, A doubly anchored surface micromachined Pirani gauge for vacuum package characterization, in: Proc. IEEE 16th Annu. Int. Conf. Micro Electro Mechanical Systems, Kyoto, Japan, January 19–23, 2003, pp. 506–509.
[2] J. Xuecheng, I. Ladabaum, F.L. Degertekin, S. Calmes, B.T. Khuri-Yakub, Fabrication and characterization of surface micromachined capacitive ultrasonic immersion transducers, J. Microelectromech. Syst. 8 (1999) 100–114.
[3] H. Kulah, Closed-loop Electromechanical Sigma–Delta Microgravity Accelerometers, University of Michigan, 2003.
[4] A.A. Seshia, M. Palaniapan, T.A. Roessig, R.T. Howe, R.W. Gooch, T.R. Schimert, S. Montague, A vacuum packaged surface micromachined resonant accelerometer, J. Microelectromech. Syst. 11 (2002) 784–793.
[5] I. Ladabaum, X. Jin, H.T. Soh, A. Atalar, B.T. Khuri-Yakub, Surface micromachined capacitive ultrasonic transducers, IEEE Trans. Ultrason. Ferroelectr. Freq. Control 45 (1998) 678–690.
[6] D. Sparks, G. Queen, R. Weston, G. Woodward, M. Putty, L. Jordan, S. Zarabadi, K. Jayakar, Wafer-to-wafer bonding of nonplanarized MEMS surfaces using solder, J. Micromech. Microeng. 11 (2001) 630–634.
[7] Y.-T. Cheng, W.-T. Hsu, K. Najafi, C.T.-C. Nguyen, L. Lin, Vacuum packaging technology using localized aluminum/silicon-to-glass bonding, J. Microelectromech. Syst. 11 (2002) 556–565.
[8] C.H. Mastrangelo, R.S. Muller, Microfabricated thermal absolute-pressure sensor with on-chip digital front-end processor, IEEE J. Solid-State Circuits 26 (12 (December)) (1991) 1998–2007.
[9] S.H. Choa, Reliability of vacuum packaged MEMS gyroscopes, J. Microelectron. Reliability 45 (2005) 361–369.
[10] J. Chae, B.H. Stark, K. Najafi, A Micromachined Pirani Gauge with Dual Heat Sinks, J. IEEE Trans. Adv. Packaging 28 (4 (November)) (2005) 619–625.
[11] Z. Gan, D. Huang, X. Wang, D. Lin, S. Liu, Getter free vacuum packaging for MEMS, Sens. Actuators A 149 (2009) 159–164.
[12] Z. Gan, D. Lin, X. Wang, C. Wang, S. Liu, H. Zhang, Vacuum measurement on vacuum packaged MEMS devices, in: 4th International Symposium on Instrumentation Science and Technology, 2006, pp. 1287–1291.
[13] J.-S. Shie, B.C.S. Chou, Y.-M. Chen, High performance Pirani vacuum gauge, J. Vacuum Sci. Technol. A: Vacuum Surf. Films 13 (1995) 2972–12972.
[14] F.T. Zhang, Z. Tang, J. Yu, R.C. Jin, A micro-Pirani vacuum gauge based on micro-hotplate technology, Sens. Actuators A 126 (2006) 300–305.
[15] P.K. Weng, J.S. Shie, Micro-Pirani vacuum gauge, Rev. Sci. Instrum. 65 (1994) 492–499.
[16] Kourosh Khosraviani, Albert M. Leung, The nanogap Pirani—a pressure sensor with superior linearity in atmospheric pressure range, J. Micromech. Microeng. 19 (2009), 045007 (8 pp.).
[17] B.C.S. Chou, Y.-M. Chen, M. Ou-Yang, J.-S. Shie, A sensitive Pirani vacuum sensor and the electrothermal SPICE modeling, in: Proceedings of the Eighth International Conference on Solid-state Sensors and Actuators Physical Sensor, Sens. Actuators A: Phys. 53 (1–3) (1996) 273–277.
[18] J.-S. Shie, Y.-M. Chen, M. Ou-Yang, B.C.S. Chou, Characterization and modeling of metal film microbolometer, IEEE J. Microelectromech. Syst. 5 (1996) 298.

Biographies

Xuefang Wang received the Ph.D. degree in mechanical engineering from Huazhong University of Science and Technology (HUST). Now he is an associate professor at School of Mechanical Science and Engineering in HUST. His major research interests include MEMS/NEMS packaging and MEMS equipments.

Chuan Liu received the B.S. degree in thermal energy and power engineering from Hefei University of Technology, Hefei, China, in 2008. He is currently working toward the Master's degree in thermal physics engineering from Huazhong University of Science and Technology, Wuhan, China. His current research interests include MEMS Vacuum Packaging, and MEMS sensors and actuators.

Zhuo Zhang received the B.S. degree in mechanical design and manufacturing in 2008 from Huazhong University of Science and Technology, Wuhan, China, where he is currently working toward the Master's degree in micro-manufacturing technology. His current research interests include MEMS/NEMS packaging and MEMS equipments.

Sheng Liu is a specially recruited professor, Director of Institute of Microsystems, Director of MOEMS Division, Wuhan National Lab of Optoelectronics, Huazhong University of Science and Technology, Wuhan, China. He obtained his Ph.D. from Stanford University in 1992. His main research interests are LED/MEMS/IC packaging, Mechanics and Sensors. He has published more than 200 technical articles and filed more than 50 patents.

Xiaobing Luo is a professor at the Huazhong University of Science and Technology (HUST), Wuhan, China. He works at the State Key Lab of Coal Combustion in School of Energy and Power Engineering and Wuhan National Lab for Optoelectronics in HUST. He received his Ph.D. in 2002 from Tsinghua University, China. From 2002 to 2005, he worked at Samsung Electronics in Korea as a senior engineer. In September 2005, he returned to China and became an associate professor. In October 2007, he was promoted to full professor. His main research interests are LED packaging, electronics packaging, heat and mass transfer. He has published more than 50 papers, applied for and owns 40 patents in USA, Korea, Japan, Europe and China.